NASA TECHNICAL NOTE

NASA TN D-7958

NASA TN D-7958

EFFECT OF FREE-STREAM TURBULENCE ON FILM COOLING

Cecil J. Marek and Robert R. Tacina

Lewis Research Center

Cleveland, Ohio 44135

NATIONAL AERONAUTICS AND SPACE ADMINISTRATION • WASHINGTON, D. C. • JUNE 1975

EFFECT OF FREE-STREAM TURBULENCE ON FILM COOLING

by Cecil J. Marek and Robert R. Tacina

Lewis Research Center

SUMMARY

Film-cooling experiments were conducted at four levels of free-stream turbulence to test the hypothesis that the film-cooling effectiveness is inversely related to the free-stream turbulence level. The hot-gas operating conditions were held constant at a temperature of 590 K, a pressure of 1 atmosphere, and a velocity of 62 meters per second. The film-cooling air was at ambient inlet temperature. The film-cooling flow rates were 2.5, 5.0, 7.5, and 10.0 percent of the total airflow.

Blockage plates with blockage areas of 0, 52, 72, and 90 percent were placed upstream of the film-cooling slot and produced axial turbulence intensities of 7, 14, 23, and 35 percent, respectively. The film-cooling effectiveness decreased as much as 50 percent as the free-stream turbulence intensity was increased from 7 to 35 percent.

A comparison was made between the turbulent mixing film-cooling correlation of Juhasz and Marek (NASA TN D-6360) and the experimental data. The agreement between the measured axial turbulence intensity and the calculated turbulent mixing coefficient was poor, the turbulent mixing coefficient being considerably less than the axial turbulence intensity. In this experiment for blockage areas of 52 and 72 percent, corresponding to average axial turbulence intensities of 14 and 23 percent, respectively, the calculated turbulent mixing coefficient was 0.05 ± 0.03.

INTRODUCTION

A film-cooling experiment was conducted over a range of turbulence intensities to test the hypothesis that the film-cooling effectiveness is inversely related to the free-stream turbulence intensity.

Juhasz and Marek (ref. 1) correlated film-cooling effectiveness data taken in a sector combustor with a turbulent mixing equation. For the combustor data, they found a value of turbulent mixing coefficient C_m as high as 0.15, whereas for film-cooling data taken in low-turbulence wind tunnels the value of C_m was calculated to be approximately 0.01. They assumed that the large difference in the correlating parameter C_m was due to the higher turbulence within the combustor, and they postulated that the turbulent mixing coefficient was equal to the hot-gas turbulence intensity. Mularz and Schultz (ref. 2) measured film-cooling data and turbulence data in a full-scale annular gas turbine combustor. They found that the turbulent mixing coefficient was only 10 percent of the turbulence intensity. The turbulent mixing coefficient was calculated to be from 0.022 to 0.04, whereas the measured axial turbulence intensity was 35 percent. Testing the correlation in a combustor is inaccurate because there are large temperature and velocity gradients making it difficult to define a single value of hot-gas temperature and velocity.

In this experiment the effect of free-stream turbulence on the film-cooling effectiveness was tested under the controlled conditions of a uniform hot-gas temperature (590 K) and a constant hot-gas velocity (62 m/sec) in a 10.5- by 37-centimeter rectangular duct. The turbulence of the hot-gas stream was varied by placing perforated blockage plates upstream of the film-cooling slot. Blockage areas of 0, 52, 72, and 90 percent were used. The film-cooling slot height was 0.63 centimeter. Ambient-temperature cooling air was used. The cooling mass flow was 2.5, 5.0, 7.5, and 10.0 percent of the total airflow.

The variation of film-cooling effectiveness with blockage area was determined. The calculated turbulent mixing coefficient C_m was compared with the measured axial and lateral turbulence intensities.

SYMBOLS

C_m	turbulent mixing coefficient defined by eq. (3)
L	integral length scale of turbulence defined by eq. (A2)
M	mass flux ratio, $\rho_s U_s / \rho_H U_H$
m_e	net mass entrained by film-cooling stream
m_s	mass flow rate of film at slot
R	autocorrelation coefficient defined by eq. (A1)
S	film slot height
T_f	film temperature
T_H	hot-gas temperature
T_s	film inlet temperature
t	time

U_H axial hot-gas stream velocity

U_s film velocity at slot

u' fluctuating axial velocity

v' fluctuating velocity normal to test plate

W width of test duct

x distance downstream of slot exit

α time delay used in autocorrelation coefficient (see eq. (A1))

η_f film-cooling effectiveness

ρ_H hot-gas density

ρ_s density of film at slot exit

τ_u axial turbulence intensity, $\sqrt{\overline{u'^2}} \times 100/U_H$, percent

τ_v lateral turbulence intensity, $\sqrt{\overline{v'^2}} \times 100/U_H$, percent

APPARATUS AND PROCEDURE

Flow System

The experiment was carried out at atmospheric pressure in a 10.5-centimeter-high by 37-centimeter-wide rectangular test section. The perforated blockage plates which were used for turbulence generators were placed 41 centimeters (approximately four duct heights) upstream of the cooling slot exit.

The airflow schematic is shown in figure 1. The temperature of the main airstream was increased to 590 K with a vitiating preheater using Jet A fuel. A large plenum was used downstream of the preheater to produce a well mixed stream at low turbulence. The hot gas then entered the test section through the perforated blockage plate.

The film-cooling air was separately metered and entered the test section through a 0.63-centimeter continuous slot which extended the complete width of the test section. The slot lip was tapered to a knife edge to prevent additional turbulence from the lip wake. The film-cooling stream was at ambient temperature and pressure.

The undersurface of the plate was insulated to minimize convective heat losses. The test plate was 0.31-centimeter-thick 304 stainless steel.

Turbulence Generators

Four levels of turbulence were generated with plates with blockage areas of 0, 52, 72, and 90 percent. The plates were placed far enough upstream of the slot exit to allow the velocity profiles to become uniform.

Since the decay rate of turbulence is inversely proportional to the mesh length (the distance from hole center to hole center) (ref. 3), the mesh length was made large to minimize the turbulence decay over the length of the film-cooled plate. The blockage plates used had two rows of seven holes each with a mesh length of 5.3 centimeters, as shown in figure 2.

Temperature Measurements

Test-plate temperatures were measured along the centerline of the test plate with Chromel-Alumel thermocouples placed 2.54 centimeters apart (fig. 3). The hot-gas temperature was determined by averaging readings from four Chromel-Alumel thermocouples placed upstream of the blockage plates. The inlet film-cooling air temperature was measured with a thermocouple placed in the inlet slot. Some heating of the cooling air (about 20 K) occurred because of convection through the test duct upstream of the slot exit between the injection tubes and the slot thermocouple (see fig. 1).

Turbulence Measurements

Turbulence was measured in the hot-gas stream at ambient temperature at the same mass flow rate as the 590 K data. Maintaining a constant mass flow rate resulted in an increase in the Reynolds number from 189 000 to 334 000 because of the decrease in viscosity with decreasing temperature. The effect was assumed to be small because of the high value of the Reynolds number. The velocity and turbulence of the stream were measured with a hot-wire anemometer which was placed in the center of the duct and traversed normal to the test plate. Hot-wire measurements were taken at the axial locations shown in figure 3. In the direction normal to the test plate, measurements were taken at 3.2, 5.7, and 8.2 centimeters from the test plate. The data reported are the averages of these three values, which were very nearly equal. The anemometer was operated at constant temperature. The tungsten hot wire was 4 micrometers in diameter by 1.25 millimeters long and was calibrated in a low-turbulence nozzle. It was assumed that operating the wire in a high-turbulence gas stream did not change its response. The signal was linearized, and the mean velocity U was measured with a direct-current voltmeter. The mean fluctuating turbulence velocities u' and v' were measured with a root-mean-square voltmeter.

At the high turbulence encountered at some conditions, the turbulence intensities measured were expected to have a relative error of 10 to 20 percent because of the nonlinear nature of the hot-wire response (ref. 4).

The alternating-current component of the hot-wire signal was tape recorded for 1 minute on an FM tape recorder. This tape was used to determine the autocorrelation coefficient R and the energy spectrum. The autocorrelation coefficient was determined by a correlator using 16 000 samples and having a 20-microsecond sampling time. The energy spectrum was determined by a narrow-band spectrum analyzer.

ANALYSIS

Film-Cooling Correlation

The film-cooling effectiveness η_f is defined as

$$\eta_f = \frac{T_H - T_f}{T_H - T_s} \tag{1}$$

From an energy balance on the film stream, Stollery and El-Ehwany (ref. 5) showed that the film-cooling effectiveness is related to the quantity of hot gas entrained by the film-cooling layer by

$$\eta_f = \frac{m_s}{m_s + m_e} \tag{2}$$

Juhasz and Marek (ref. 1) assumed that the entrainment rate is proportional to the hot-gas mass flux and is given by

$$m_e = C_m \rho_H U_H x W \tag{3}$$

The turbulent mixing coefficient C_m was postulated to be equal to the turbulence intensity. The amount of hot gas entrained by the film-cooling stream can be calculated from equation (3) for various values of the turbulent mixing coefficient.

Equations (2) and (3) can be combined to give

$$\eta_f = \frac{1}{1 + C_m \frac{x}{MS}} \tag{4}$$

Values of the turbulent mixing coefficient C_m were calculated for various conditions from the experimental wall temperatures by using equation (4). The values of C_m were then compared with the free-stream turbulence intensities.

Estimated Accuracy of Experimental Film-Cooling Data

In the calculation of the film-cooling effectiveness, it is necessary to know the film-cooling stream temperature T_f at each axial location. For an adiabatic, film-cooled wall, the film stream temperatures and wall temperatures are equal. For calculation of the film-cooling effectiveness in this experiment, it was assumed that the local film-cooling stream temperatures were equal to the wall temperatures. The maximum difference between the film-cooling stream temperatures and the wall temperatures, due to axial wall conduction, was estimated to be 7 K. This estimate was made by using the hot-gas mass flux to calculate the convective heat-transfer coefficient between the film stream and the wall.

No correction was applied to the data because of the uncertainty in the value of the convective heat-transfer coefficient at low values of x/S and because the correction would have been of the same order of magnitude as the uncertainties in the temperature data. It was estimated that variations in the hot-gas temperature of ±5 K were present. For the hot-gas temperature of 590 K and the inlet film-cooling temperature of 300 K, the sum of the maximum estimated wall-conduction correction and the uncertainty in the experimental temperature data would result in a maximum deviation in the film-cooling effectiveness of 0.04.

RESULTS AND DISCUSSION

The film-cooling effectiveness was determined at four levels of free-stream turbulence. Plates with blockage areas of 0, 52, 72, and 90 percent were placed in the hot-gas stream and produced turbulence levels of 7, 14, 23, and 35 percent, respectively.

The effect of blockage area on the film-cooled test-plate temperatures is discussed first and then the relation between the turbulence intensity and the turbulent mixing coefficient C_m is discussed.

Test-Plate Temperature

The film-cooled test-plate temperatures are shown in figure 4 as a function of downstream distance with blockage area as a parameter. The results show an increase in plate temperatures with increasing blockage, which was attributed to higher entrainment rates of hot gas by the film-cooling stream. Test-plate temperatures increased by 70 K when the blockage area increased from 0 to 90 percent. The test-plate temperature at the 21.28-centimeter location was below the 18.74-centimeter plate temperature because of wall conduction to the plate supports. The experimental data are given in table I.

When the blockage plates were added, there was a change in velocity profiles. The ambient-temperature velocity profiles 0.63 centimeter downstream of the slot exit as determined from the hot-wire data are shown in figure 5. With no blockage the profile was center peaked. With a blockage plate in the flow, the profile was inverted and was center deficient. For the four configurations the maximum velocity was only 20 percent higher than the mean velocity, which indicates a relatively uniform velocity profile. The profiles for the three blockage plates had the same shape and differed from each other by less than 10 percent. With similar hot-gas profiles the 20-percent change in hot-gas velocity would not by itself account for the differences in test-plate temperatures shown in figure 4.

Film-Cooling Effectiveness

The temperature data were converted to the film-cooling effectiveness η_f by using equation (1) and assuming that the wall temperature and the film temperature were equal. The film-cooling effectiveness is plotted as a function of the downstream distance parameter x/MS in figure 6 with blockage as a parameter. This plot takes into account the small changes in flow rates from run to run.

As the blockage area was increased, the film-cooling effectiveness decreased for a given value of x/MS. As the blockage was increased from 0 to 90 percent, the film-cooling effectiveness decreased by as much as 0.3.

Figure 7 shows a comparison between the experimental data and the turbulent mixing correlation of reference 1 given by

$$\eta_f = \frac{1}{1 + C_m \frac{x}{MS}} \tag{4}$$

The data show considerable deviation from the turbulent mixing correlation if a constant value of C_m over the whole test plate is assumed. If a constant value of C_m is taken for each blockage plate, the deviation between the correlation and the film-cooling effectiveness is ±30 percent.

The value of C_m inferred from the experimental data by using equation (4) is plotted as a function of x/MS in figure 8. The figure shows that C_m is not only a function of blockage but also a function of x/MS. At the slot exit for high cooling flows, small errors in test-plate temperature could produce large errors in C_m. The value of C_m varied by ±50 percent over the length of the test plate. The average turbulent mixing coefficient C_m was as follows:

Blockage, percent	Average turbulent mixing coefficient, C_m
0	0.025±0.01
52	0.04±0.02
72	0.05±0.03
90	0.1±0.05

Increasing the blockage did increase C_m and resulted in a more rapid degradation in the film-cooling effectiveness.

The turbulent mixing coefficient C_m at the 11.1-centimeter location is cross plotted as a function of cooling mass flow in figure 9. As the velocity ratio increased toward 1, C_m decreased, which indicates a decrease in the hot-gas entrainment by the film-cooling stream with an accompanying increase in the film-cooling effectiveness. From the data of figure 9, which are for an x/S of 17.6, it appears that a velocity ratio effect existed and was more dominant at higher turbulence levels. The effect may have been related to the increase in momentum of the cooling stream.

Kacker and Whitelaw (ref. 6) found an increase in the film-cooling effectiveness as the velocity ratio approached 1. For their data the x/S values had to be at least 25 for the effect to be present. Their data showed a change in C_m of 0.005, from 0.015 to 0.010, as the velocity ratio went from 0.5 to 1.0. They attributed the decrease in mixing to the elimination of velocity shear in the mixing region.

In the work of reference 1 the film-cooling effectiveness did not increase as the slot height was decreased at constant cooling flow to allow the velocity ratio to approach 1. However, the film degradation was already very high, and the effect may have been small.

Relation Between Turbulent Mixing Coefficient and Turbulence Intensity

The axial turbulence intensity was measured in the center of the duct at various axial locations to determine whether a relation exists between the turbulence intensity and the turbulent mixing coefficient. The turbulence intensities were measured at ambient temperature, as discussed in the section APPARATUS AND PROCEDURE. The average turbulence intensity ranged from 7 to 35 percent, whereas the turbulent mixing coefficient ranged from 0.02 to 0.14. Figure 10 shows the variation of the axial turbulence intensity with distance. There was a relative variation of ±10 percent in the data from day to day. The higher blockage resulted in a higher turbulence intensity. Also the turbulence intensity decreased with increasing distance from the blockage plate. The average turbulence intensities above the test area were 7, 14, 23, and 35 percent for blockage areas of 0, 52, 72, and 90 percent, respectively.

A plot of C_m as a function of the turbulence intensity is shown in figure 11. The value of C_m was much lower than the turbulence intensity. There was a trend toward higher values of C_m at higher values of the turbulence intensity. The relation might be expressed by

$$C_m = (0.25 \pm 0.15) \frac{\tau_u}{100} \tag{5}$$

In the work of reference 1, it was postulated that the rate of mixing should be related to the lateral fluctuating velocity normal to the test plate v' by the expression

$$C_m = \frac{\tau_v}{100} \equiv \frac{\sqrt{\overline{v'^2}}}{U_H} \tag{6}$$

In this experiment, in an effort to determine the magnitude of the lateral turbulence intensity, the wire was oriented parallel to the axial velocity. In this direction it would be less sensitive to fluctuations in the axial velocity. One of the support prongs of the hot wire was positioned upstream of the wire and influenced the flow which the wire saw; however, the lateral turbulence intensity should have been an indication of how isotropic the flow was. The wake of the support prong would result in values of intensity somewhat higher than the true value.

Figure 12 shows the mean lateral turbulence intensity normalized by the mean axial velocity. The lateral turbulence intensity was approximately 50 percent of the axial turbulence intensity, which indicates that the turbulence was highly nonisotropic. Plotting C_m as a function of the lateral turbulence intensity still resulted in considerable scatter, as shown in figure 13. The value of C_m was lower than the value of the lateral turbulence intensity.

Equation (6) is an oversimplification of the problem. A general relation for the turbulent mixing coefficient would be much more complex and would probably involve the turbulence of both the film-cooling stream and the hot-gas stream and the mixing generated by the mixing shear layer between the film-cooling stream and the hot-gas stream. In this experiment the slot exit axial and lateral turbulence intensities defined in terms of the slot exit velocity were measured to be 20 and 10 percent, respectively, at the slot exit. The upstream hot-gas velocity profile also significantly affected the mixing along the test plate.

The mixing which occurs at high turbulence levels in nonisotropic turbulence is not well understood. The scale of turbulence and the spectrum of turbulence should be important parameters in characterizing the mixing. Further analysis of the turbulence measurements, including the autocorrelation coefficient, integral scale of turbulence, and energy spectrum, is presented in the appendix.

CONCLUDING REMARKS

Measurements showed that the film-cooling effectiveness decreases as the free-stream turbulence intensity increases. The present test section was located four duct heights downstream of the blockage, far enough downstream to be equivalent to a turbine inlet station. Gas turbine combustors usually are designed with 50- to 75-percent blockage. The data of this report indicate that the turbulent mixing coefficient which would be applicable for turbine cooling downstream of typical combustors ranges from 0.03 to 0.08. In the work of references 7, 8, and 9, where data were taken in a combustor exhaust stream, the turbulent mixing coefficient was 0.03, 0.05, and 0.05, respectively, which is within the range found in this experiment.

Film-cooling data which have been measured in combustors have shown values of turbulent mixing coefficients ranging from 0.02 to 0.15. In the work of references 10 and 11 turbulent mixing coefficients within the primary zone of 0.03 and 0.02 were calculated by comparison of equation (4) with experimental liner temperatures after corrections were made for convection and radiation. A value of the turbulent mixing coefficient within the dilution zone of 0.15 was obtained in the study of reference 1, and values from 0.022 to 0.04 were obtained in the study of reference 2. Some of the differences in C_m values were due to the fact that the uncooled wall temperature was used as the hot-gas temperature in the work of reference 1, whereas the mean combustor exit hot-gas temperature was used in the work of reference 2.

It is difficult to predict film temperatures with a one-dimensional model where large gradients in velocity and temperature are present and a two- or three-dimensional numerical model needs to be incorporated. However, the one-dimensional model is useful for estimation of cooling flows by using typical values for the turbulent mixing coefficient as applicable from the references cited. In addition, as shown in references 2 and 11, after a value for the turbulent mixing coefficient is determined from initial experiments, this value can be used to calculate the effect of changes in the cooling flow or combustor operating conditions.

SUMMARY OF RESULTS

Film-cooled wall temperatures were measured downstream of turbulence-producing blockage plates within a 10.5-centimeter-high by 37-centimeter-wide rectangular duct. Blockage areas of 0, 52, 72, and 90 percent were used. The plates were placed four duct heights upstream of the film-cooled wall and produced average axial turbulence intensities of 7, 14, 23, and 35 percent.

Film-cooling experiments were conducted with a hot-gas temperature of 590 K and an ambient film-cooling air temperature. The hot-gas velocity was 62 meters per second, and the film-cooling airflow rates were 2.5, 5.0, 7.5, and 10.0 percent of the total airflow. The following results were obtained:

1. High turbulence resulted in more rapid degradation of the film-cooling layer and higher test-plate temperatures. The film-cooling effectiveness decreased as much as 50 percent as the axial turbulence intensity was increased from 7 to 35 percent.

2. The difference between the film-cooling effectiveness predicted from the turbulent mixing correlation by assuming a constant value of the turbulent mixing coefficient and the experimental data over the test plate was ±30 percent.

3. For combustors with 50- to 75-percent blockage, a value of the turbulent mixing coefficient applicable at the turbine station would be 0.05±0.03.

4. The correlation between the turbulent mixing coefficient and the axial turbulence intensity was poor. The turbulent mixing coefficient was between 10 and 40 percent of the axial turbulence intensity. However, a trend existed toward higher turbulent mixing coefficients at higher turbulence.

Lewis Research Center,
National Aeronautics and Space Administration,
Cleveland, Ohio, January 13, 1975,
505-03.

APPENDIX - MEASUREMENT OF TURBULENCE PARAMETERS

The net entrainment by the film stream should depend on the scale and spectrum of turbulence. To document the turbulence characteristics, several further measurements were made including the autocorrelation coefficient R and the energy spectrum. The autocorrelation coefficient, which gives an indication of the periodicity of the eddies, is defined as

$$R(\alpha) = \frac{1}{\overline{u'^2}} \lim_{t \to \infty} \frac{1}{t} \int_0^t u'(t)u'(t - \alpha)\, dt \tag{A1}$$

It is presented in figure 14. The function follows the typical exponential decay characteristic of random turbulence. Figures 14(a) and (b) show the variation of the autocorrelation coefficient with changes in blockage and downstream distance, respectively. The coefficient did not change significantly with either variation.

The integral scale of turbulence, which gives an indication of the mean eddy size, is defined as

$$L = U_H \int_0^\infty R(\alpha)\, d\alpha \tag{A2}$$

The value of the integral was determined for each configuration by integrating to the first negative value of the autocorrelation coefficient R as was done in the work of reference 12. The integral scale of turbulence with the blockage plates was equal to approximately one-half the mesh length and increased with distance from the slot (fig. 15). The three plates had the same integral scale of turbulence. With no blockage plate present the integral scale was equal to 0.5 times the duct height and decreased with distance from the slot. Laufer (ref. 13) found the integral scale to be 0.4 times the channel height.

The energy spectrum of the turbulence was also determined and plotted in figure 16. Considerable energy existed in the low-frequency range below 1000 hertz. The spectrum was very broad, which indicates the random nature of the turbulence. Dominant frequencies appeared at 6000 and 12 000 hertz, possibly as a result of instabilities in the anemometer electronics (fig. 16(c)). The spectrum above 2000 hertz followed the universal turbulent equilibrium -5/3 decay law (ref. 4). Figure 16(b) shows that the spectrum of lateral turbulence above 3000 hertz was very close to the axial turbulence spectrum, which indicates that the small-scale turbulence was nearly isotropic.

In figure 16(a), the spectrum comparing the various blockage plates indicates that the energy at all frequencies was being increased as the blockage was increased.

REFERENCES

1. Juhasz, Albert J.; and Marek, Cecil J.: Combustor Liner Film Cooling in the Presence of High Free-Stream Turbulence. NASA TN D-6360, 1971.
2. Mularz, Edward J.; and Schultz, Donald F.: Measurements of Liner Cooling Effectiveness Within a Full-Scale Double-Annular Ram-Induction Combustor. NASA TN D-7689, 1974.
3. Kistler, A. L.; and Vrebalovich, T.: Grid Turbulence at Large Reynolds Numbers. J. Fluid Mech., vol. 26, pt. 1, Sept. 1966, pp. 37-47.
4. Hinze, J. O.: Turbulence. McGraw-Hill, New York, 1959.
5. Stollery, J. L.; and El-Ehwany, A. A. M.: A Note on the Use of a Boundary-Layer Model for Correlating Film-Cooling Data. Int. J. Heat and Mass Transfer, vol. 8, no. 1, Jan. 1965, pp. 55-65.
6. Kacker, S. C.; and Whitelaw, J. H.: The Effect of Slot Height and Slot-Turbulence Intensity on the Effectiveness of the Uniform Density, Two-Dimensional Wall Jet. ASME, Paper 68-HT-4, Nov. 1968.
7. Marek, Cecil J.; and Juhasz, Albert J.: Simultaneous Film and Convection Cooling of a Plate Inserted in the Exhaust Stream of a Gas Turbine Combustor. NASA TN D-7156, 1973.
8. Marek, Cecil J.: Effect of Pressure on Tangential-Injection Film Cooling in a Combustor Exhaust Stream. NASA TM X-2809, 1973.
9. Tacina, Robert; and Marek, Cecil J.: Film Cooling in a Combustor Operating at Fuel-Rich Exit Conditions. NASA TN D-7513, 1974.
10. Norgren, Carl T.: Comparison of Primary-Zone Combustor Liner Wall Temperatures With Calculated Predictions. NASA TM X-2711, 1973.
11. Ingebo, Robert D.; Doskocil, Albert J.; and Norgren, Carl T.: High Pressure Performance of Combustion Segments Utilizing Pressure-Atomizing Fuel Nozzles and Air Swirlers for Primary-Zone Mixing. NASA TN D-6491, 1971.
12. Howard, Charles D.; and Laurence, James C.: Measurement of Screen Size Effects on Intensity, Scale, and Spectrum of Turbulence in a Free Subsonic Jet. NASA TN D-297, 1960.
13. Laufer, J.: Investigation of Turbulent Flow in a Two Dimensional Channel. NACA TN 2123, 1950.

TABLE I. - EXPERIMENTAL DATA

Blockage area, percent	Hot-gas flow rate, kg/sec	Hot-gas temperature, K	Cooling flow, kg/sec	Cooling flow, percent	Cooling air temperature, K	Downstream distance, cm								
						0.95	3.50	6.04	8.58	11.12	13.66	16.20	18.74	21.28
						Test-plate temperature, K								
0	1.45	595	0	0	529	557	573	577	578	579	579	579	577	571
	1.44	595	.039	2.62	338	355	385	426	460	482	496	506	511	509
	1.46	594	.079	5.16	315	324	335	353	379	404	424	440	451	453
	1.45	592	.119	7.62	306	314	326	341	360	379	396	411	422	423
	1.45	594	.161	9.97	298	306	318	332	346	358	370	381	389	389
52	1.45	594	0.039	2.60	345	376	436	479	504	519	527	533	535	531
	1.46	588	.077	5.04	318	328	347	379	413	438	455	468	476	475
	1.46	587	.120	7.61	309	317	330	350	378	402	422	436	446	445
	1.42	593	.156	9.93	299	306	317	332	349	365	380	392	402	403
72	1.45	596	0	0	575	584	590	590	590	590	589	---	587	580
	1.46	589	.036	2.42	358	400	467	503	523	534	541	---	545	540
	1.47	581	.076	4.95	329	339	365	406	441	464	479	---	495	494
	1.45	589	.118	7.54	319	325	340	365	398	424	443	---	465	465
	1.46	590	.163	10.00	311	315	324	341	364	387	405	---	429	432
90	1.48	584	0	0	592	592	593	592	592	591	591	590	587	579
	1.48	586	.044	2.87	354	401	466	507	531	545	553	557	558	554
	1.49	585	.088	5.57	329	352	391	434	470	493	508	518	523	519
	1.48	586	.124	7.77	315	324	345	379	417	445	466	480	489	488
	1.48	590	.163	9.89	308	315	331	354	385	412	433	450	460	458

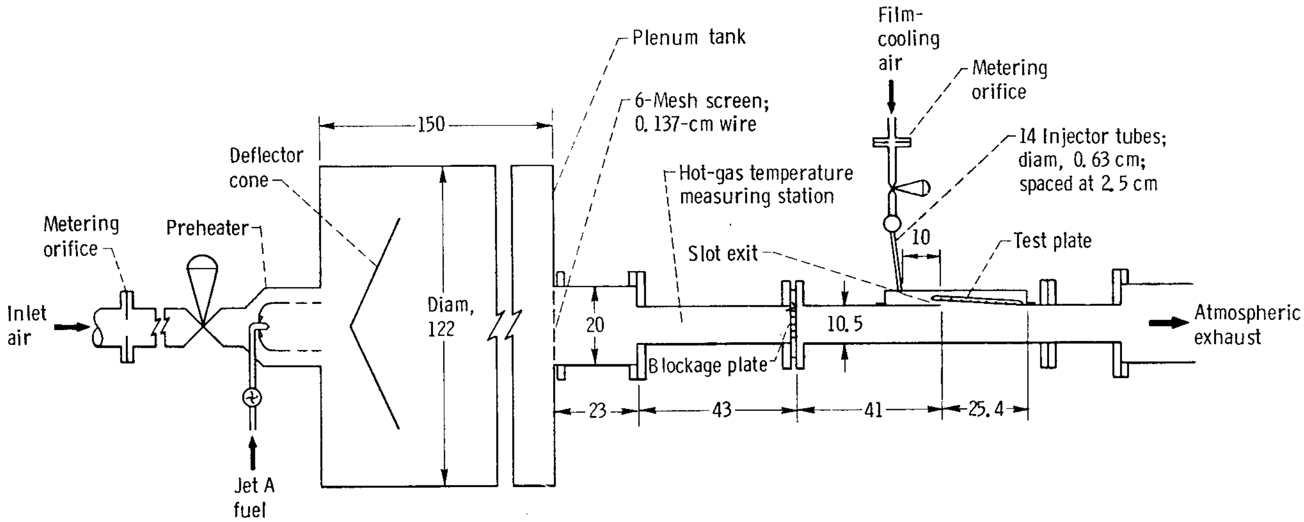

Figure 1. - Airflow schematic showing test section. Width of test section, 37 centimeters. (Dimensions are in centimeters.)

Jet wakes are probably forward at 8 L/Ds or 16 cm

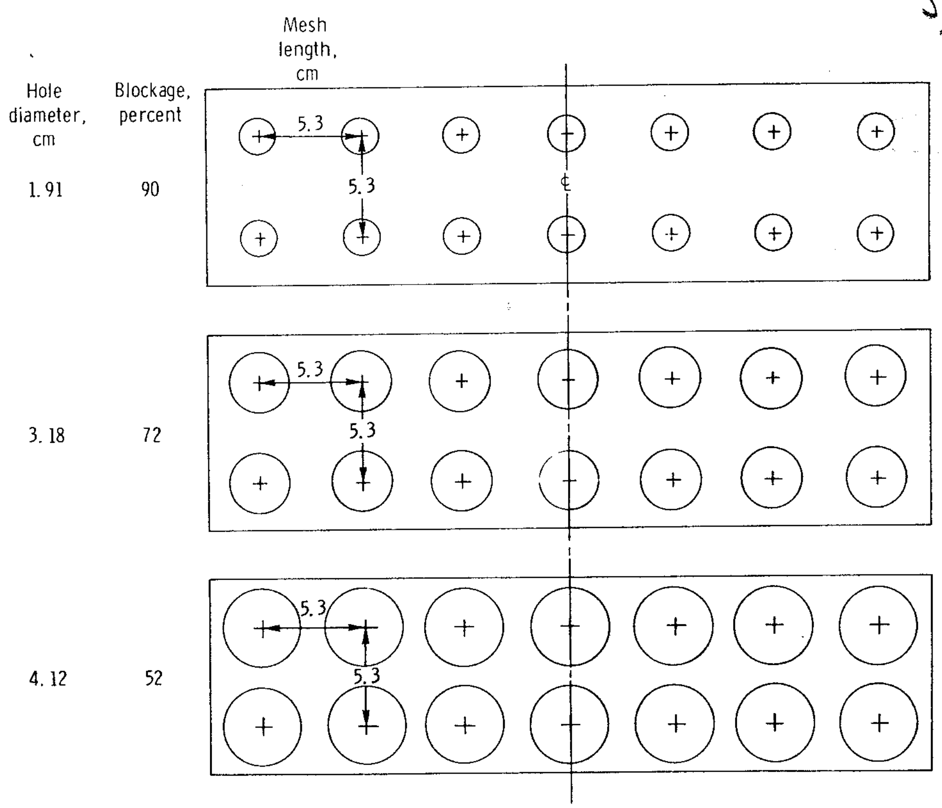

Figure 2. - Hole geometry of blockage plates.

$$\frac{A_{open}}{A_{Duct}} = \text{Blockage}$$

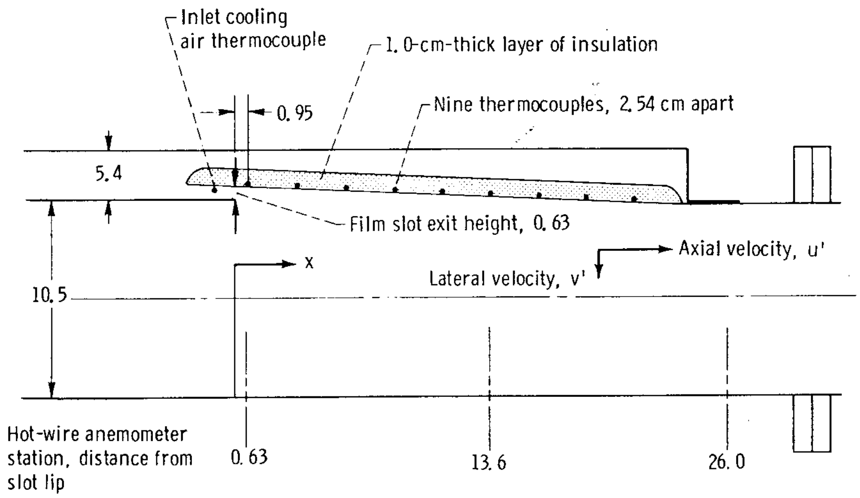

Figure 3. - Locations of test-plate thermocouples and anemometer stations. (Dimensions are in centimeters.)

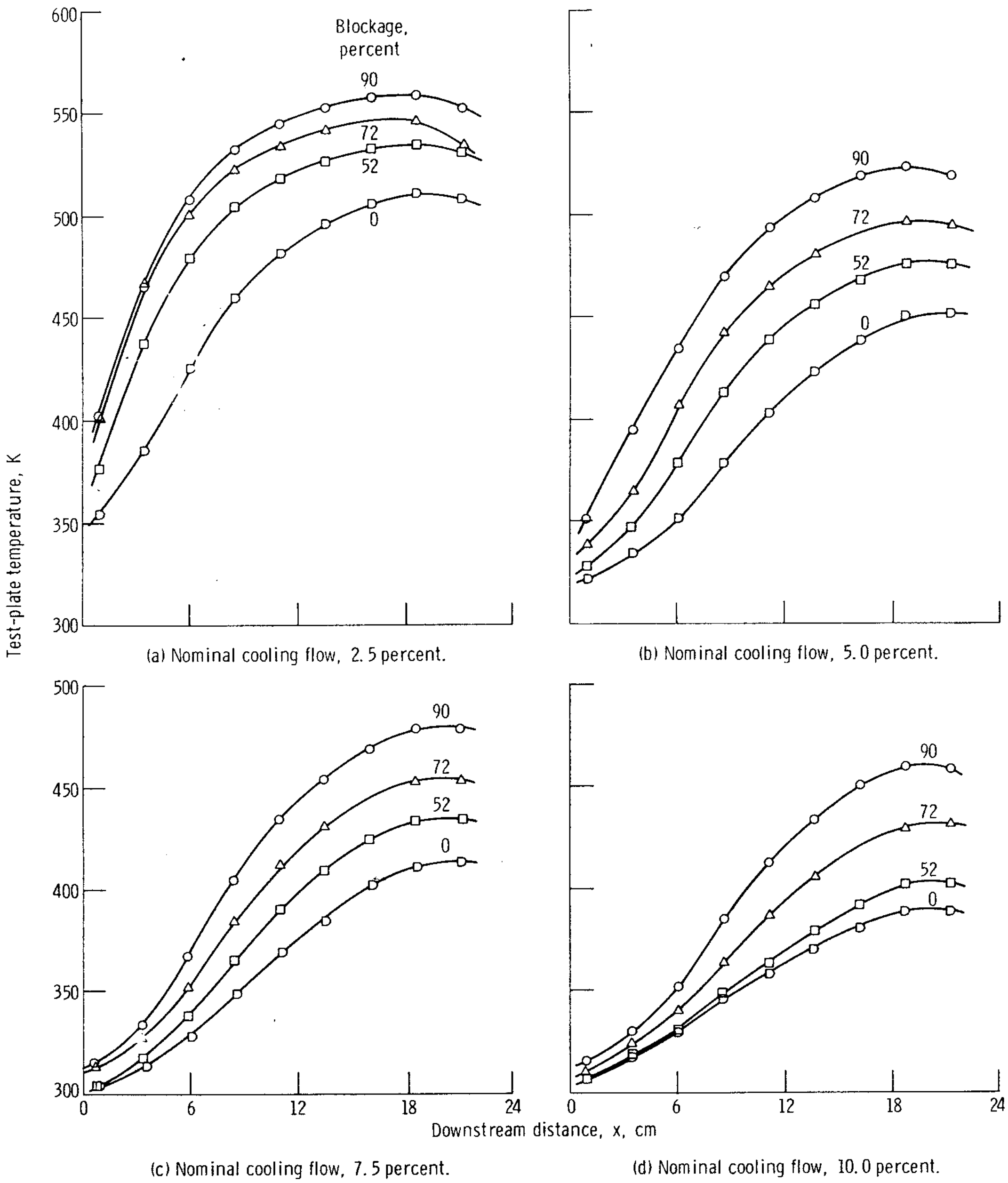

Figure 4. - Wall temperature as function of downstream distance at various blockages of hot-gas stream. Hot-gas temperature, 590 K.

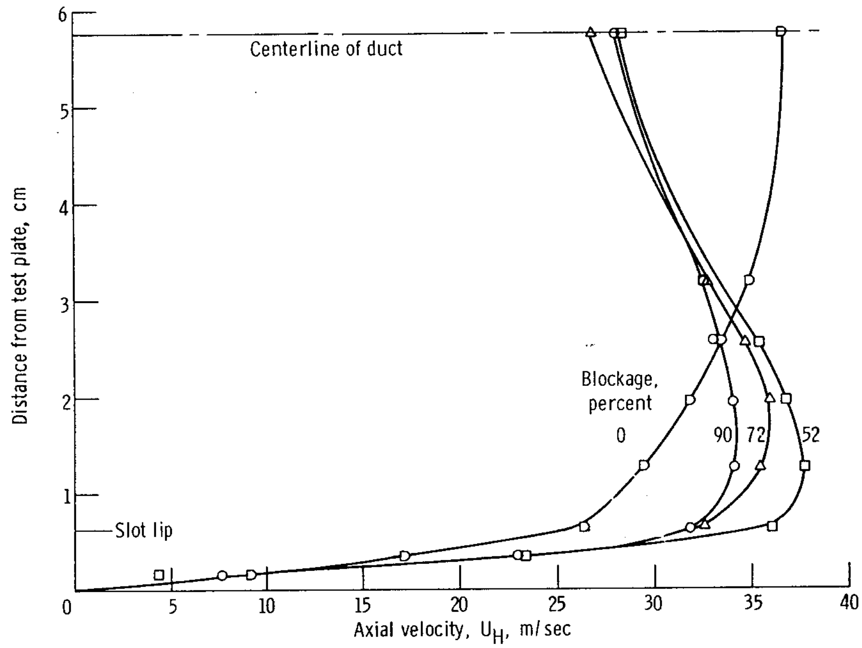

Figure 5. - Profile of axial velocity 0.63 centimeter downstream of slot lip. Nominal temperature, 290 K; mean axial velocity, 30 meters per second.

$$\frac{\overline{T_H} - T_W}{\overline{T_H} - T_C}$$

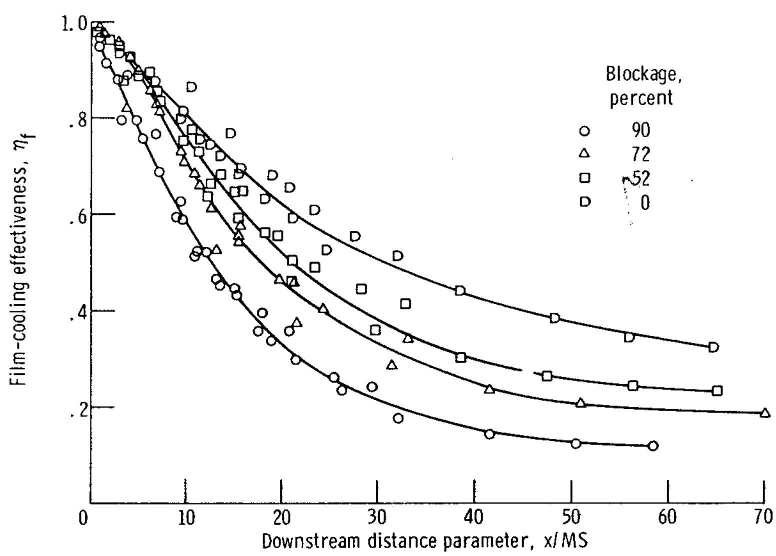

Figure 6. - Effect of blockage area on film-cooling effectiveness.

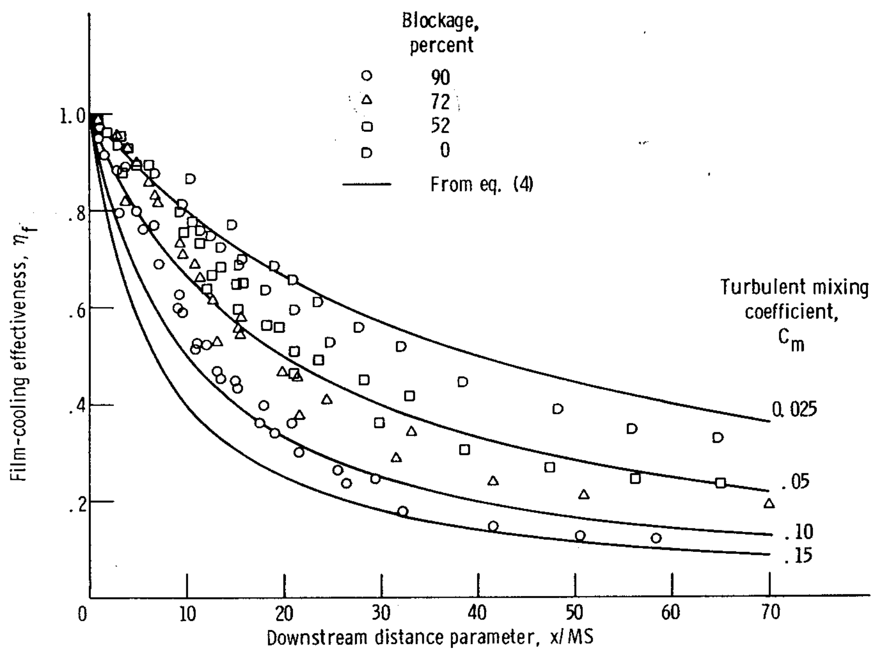

Figure 7. - Comparison of turbulent mixing film-cooling correlation with experimental data.

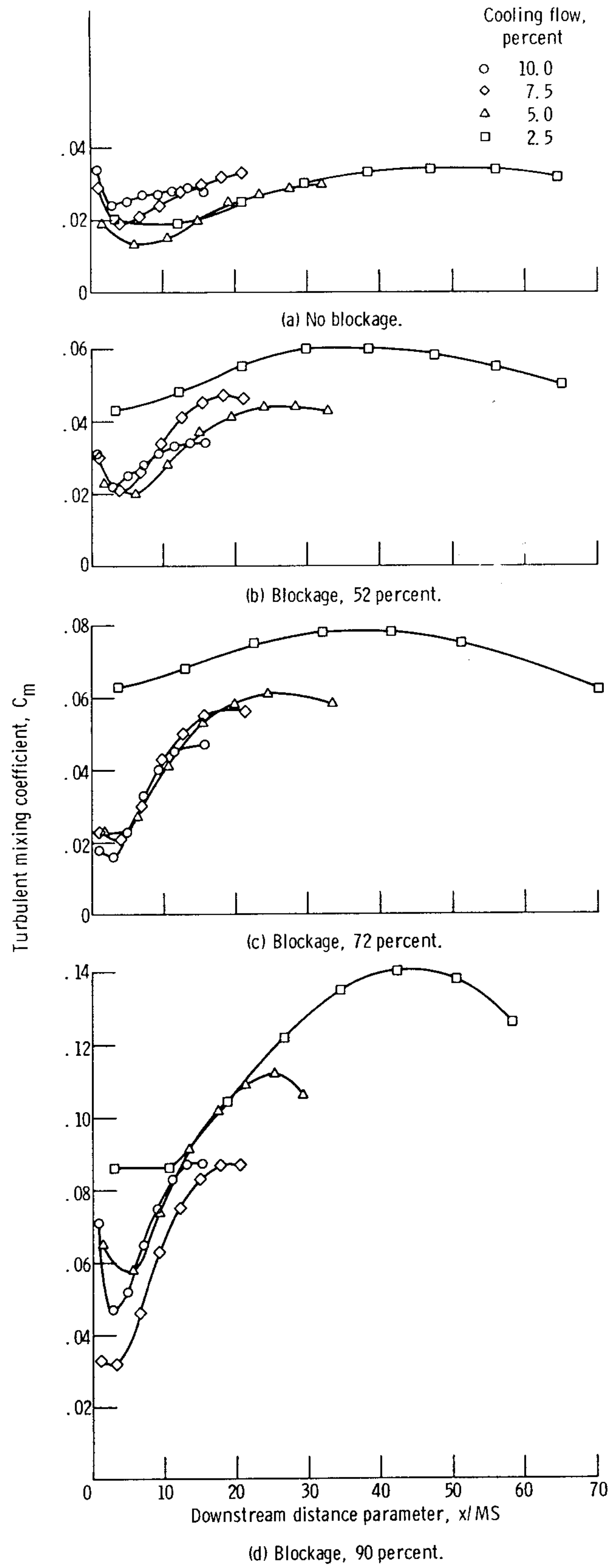

Figure 8. - Variation of turbulent mixing coefficient with downstream distance parameter.

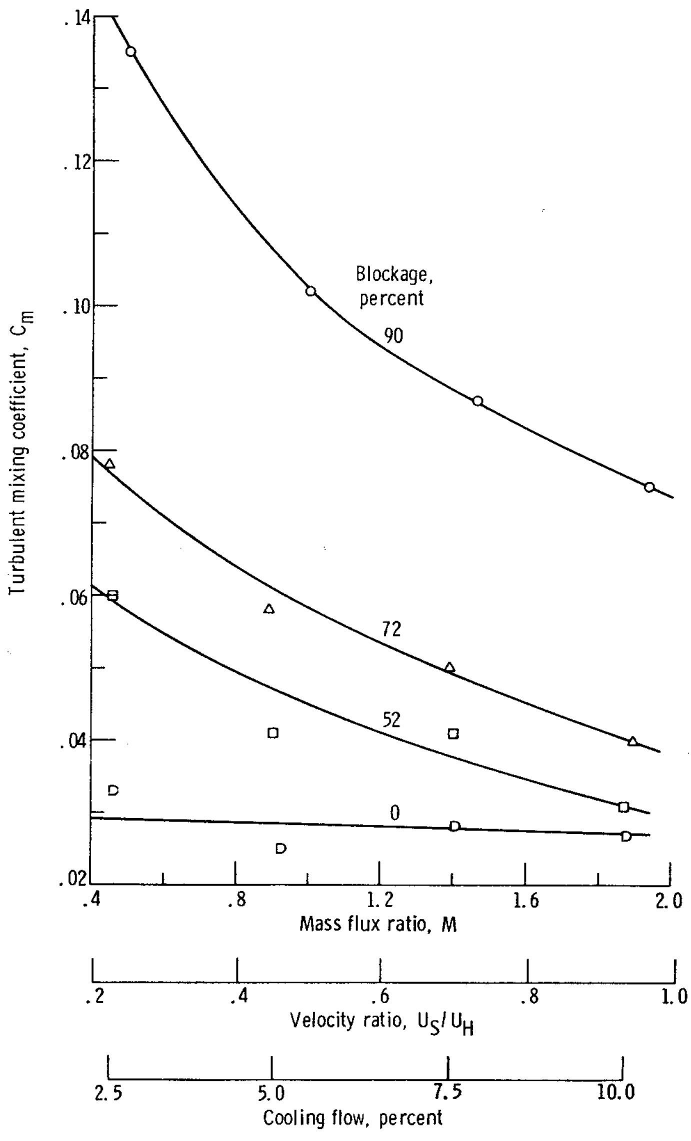

Figure 9. - Effect of cooling mass flux ratio on turbulent mixing coefficient at constant hot-gas flow rate. Downstream distance, 11.1 centimeters.

60%

what do you think these values project to 60%?

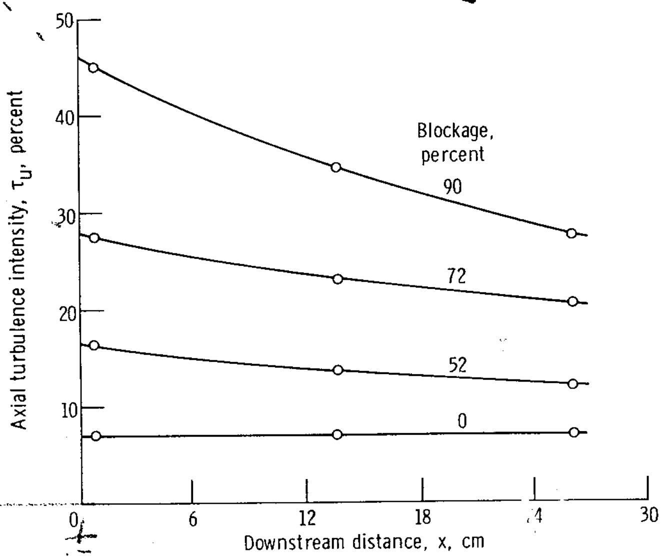

Perforated Plate 41 cm upstream See Fig 1

slot exit

Figure 10. - Axial turbulence intensity as function of downstream distance from slot exit.

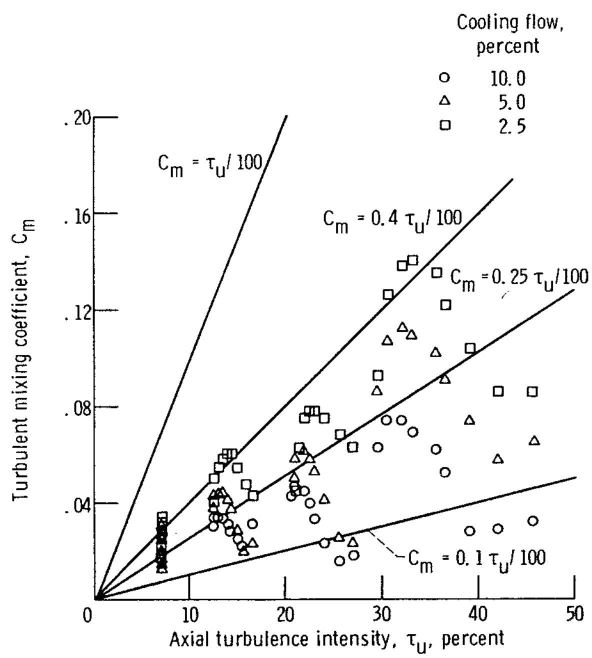

Figure 11. - Comparison of axial turbulence intensity with turbulent mixing coefficient.

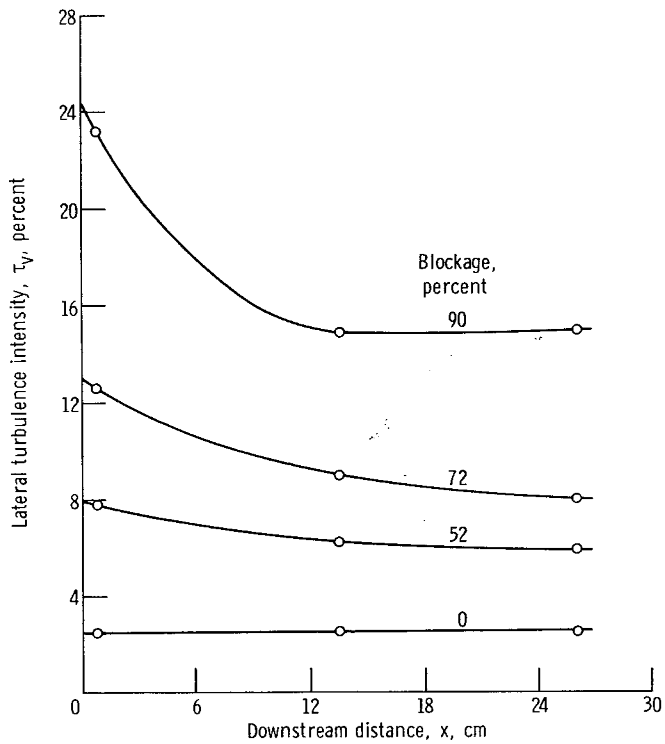

Figure 12. - Lateral turbulence intensity as function of downstream distance from slot exit.

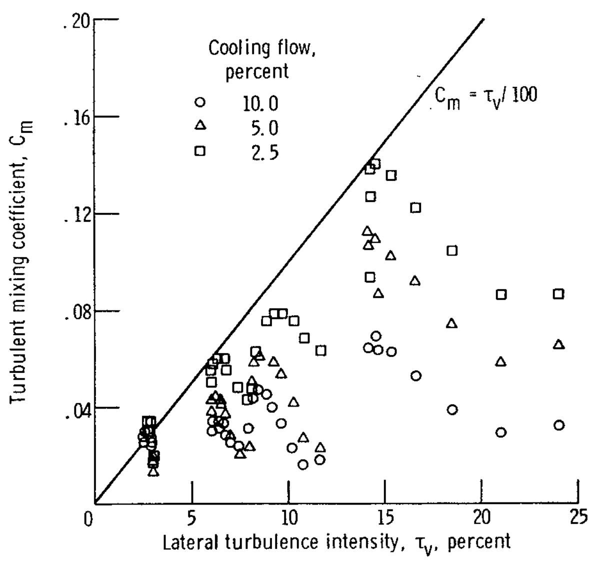

Figure 13. - Comparison of lateral turbulence intensity with turbulent mixing coefficient.

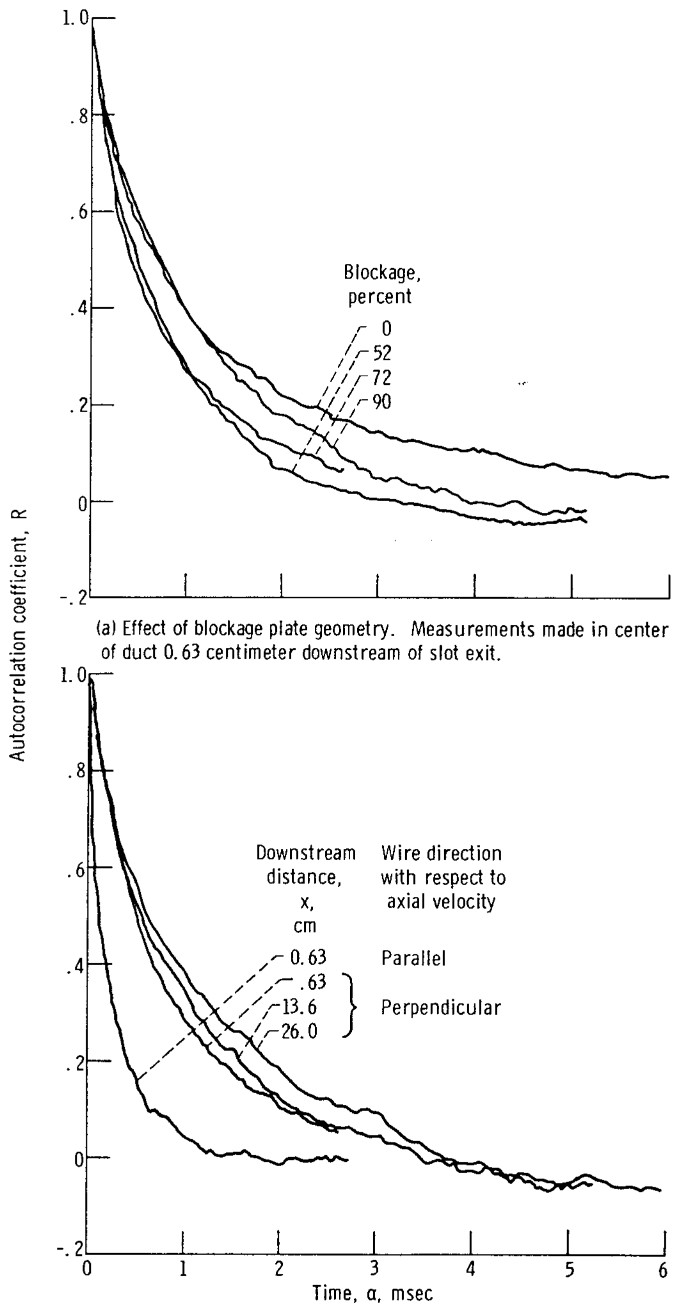

(a) Effect of blockage plate geometry. Measurements made in center of duct 0.63 centimeter downstream of slot exit.

(b) Effect of downstream distance. Measurements made in center of duct; blockage, 72 percent.

Figure 14. - Autocorrelation function. Ambient temperature; duct velocity, 30 meters per second.

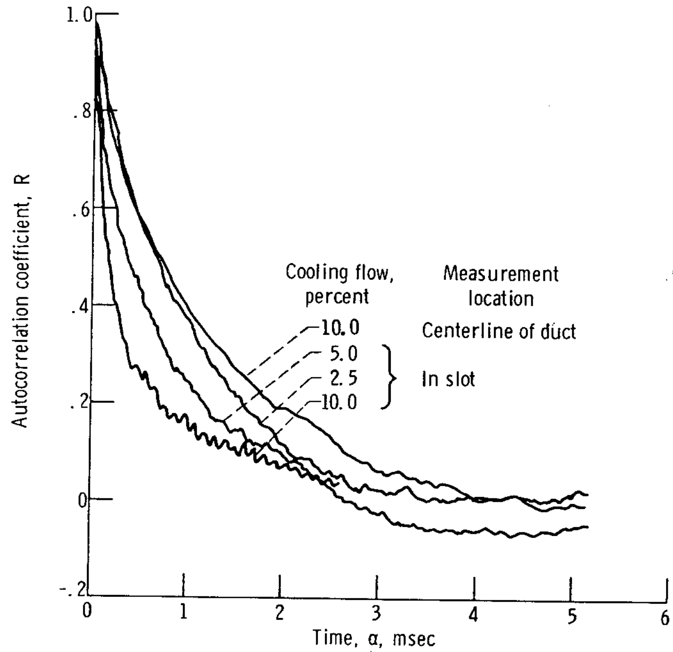

(c) Effect of cooling flow rate. Measurements made 0.3 centimeter above test plate at distance of 0.63 centimeter downstream of slot exit; blockage, 90 percent.

Figure 14. - Concluded.

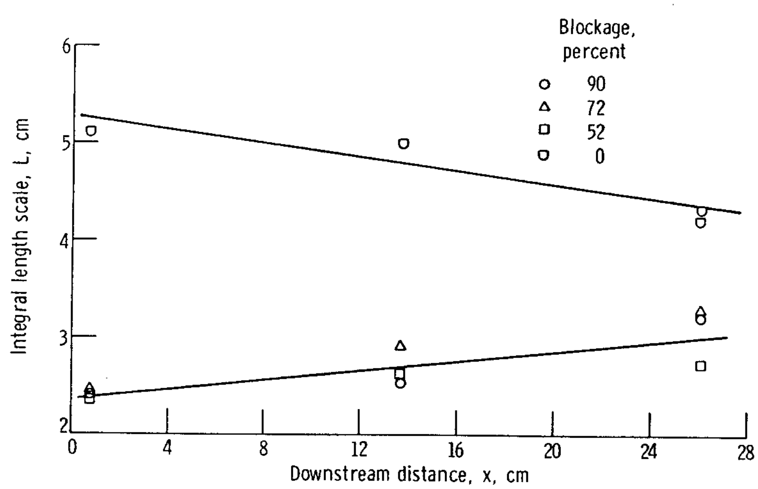

Figure 15. - Integral scale of turbulence at centerline of duct.

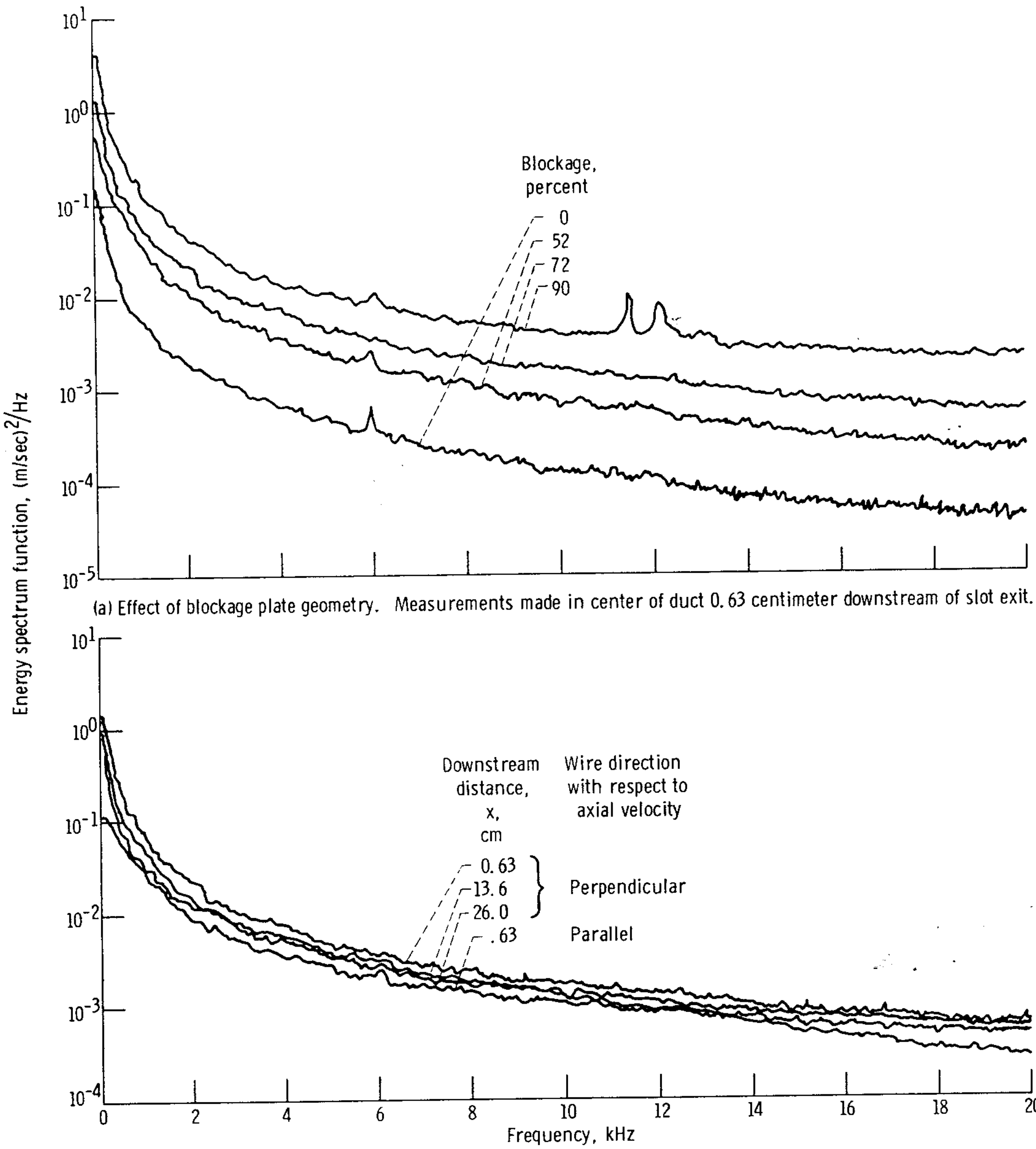

(a) Effect of blockage plate geometry. Measurements made in center of duct 0.63 centimeter downstream of slot exit.

(b) Effect of downstream distance. Measurements made in center of duct; blockage, 72 percent.

Figure 16. - Energy spectrum. Ambient temperature; duct velocity, 30 meters per second.

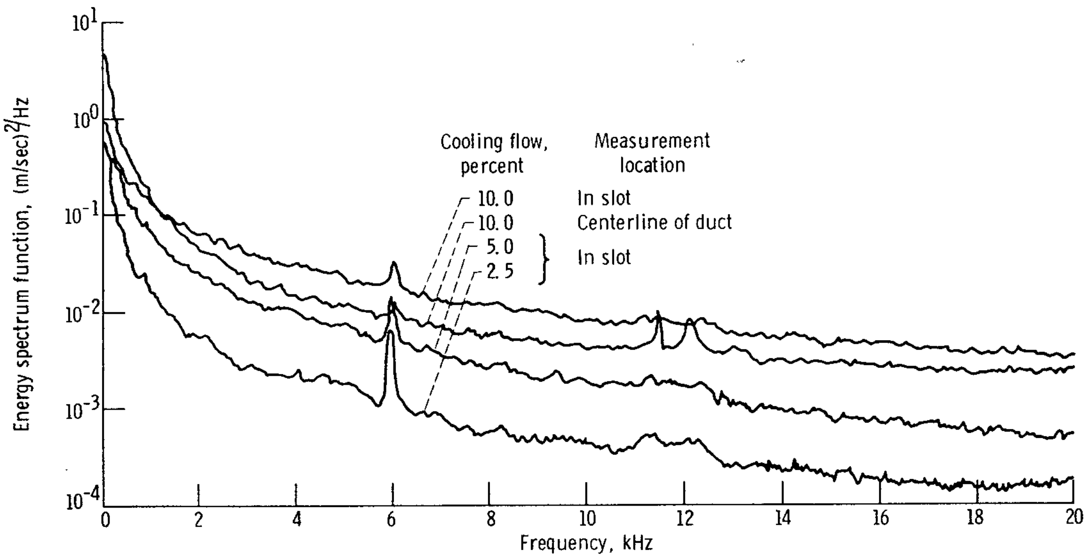

(c) Effect of cooling flow rate. Measurements made 0.3 centimeter above test plate at distance of 0.63 centimeter downstream of slot exit; blockage, 90 percent.

Figure 16. - Concluded.

1. Report No.	2. Government Accession No.	3. Recipient's Catalog No.
NASA TN D-7958		

4. Title and Subtitle	5. Report Date
EFFECT OF FREE-STREAM TURBULENCE ON FILM COOLING	June 1975
	6. Performing Organization Code

7. Author(s)	8. Performing Organization Report No.
Cecil J. Marek and Robert R. Tacina	E-8188
	10. Work Unit No.
9. Performing Organization Name and Address	505-03
Lewis Research Center National Aeronautics and Space Administration Cleveland, Ohio 44135	11. Contract or Grant No.

12. Sponsoring Agency Name and Address	13. Type of Report and Period Covered
National Aeronautics and Space Administration Washington, D.C. 20546	Technical Note
	14. Sponsoring Agency Code

15. Supplementary Notes

16. Abstract

Film-cooling experiments were conducted at four levels of free-stream turbulence to test the hypothesis that the film-cooling effectiveness is inversely related to the free-stream turbulence level. The hot-gas operating conditions were held constant at a temperature of 590 K, a pressure of 1 atmosphere, and a velocity of 62 m/sec. The film-cooling air was at ambient inlet temperature. The film-cooling flow rates were 2.5, 5.0, 7.5, and 10.0 percent of the total airflow. Blockage plates with blockage areas of 0, 52, 72, and 90 percent were placed upstream of the film-cooling slot and produced axial turbulence intensities of 7, 14, 23, and 35 percent, respectively. The film-cooling effectiveness decreased as much as 50 percent as the free-stream turbulence intensity was increased from 7 to 35 percent. The value of the turbulent mixing coefficient used in previous work was compared with the axial turbulence intensity. The turbulent mixing coefficient was 10 to 40 percent of the axial turbulence intensity.

17. Key Words (Suggested by Author(s))	18. Distribution Statement
Film cooling Combustor cooling Turbulence	Unclassified - unlimited STAR category 34 (rev.)

19. Security Classif. (of this report)	20. Security Classif. (of this page)	21. No. of Pages	22. Price*
Unclassified	Unclassified	28	$3.75

* For sale by the National Technical Information Service, Springfield, Virginia 22151